

# Impact Assessment of Vehicle-to-grid Technology in LFC of Multi-area Solar-thermal Power System

Pushpa Gaur \*‡, Nirmala Soren \*, Debashish Bhowmik \*\*

\* Department of Electrical Engineering, National Institute of Technology Silchar, Assam, India

\*\* Department of Electrical Engineering, Tripura Institute of Technology Narsingarh, Agartala, Tripura, India

(pushpa.electrical@gmail.com, nirmala@ee.nits.ac.in, debashish.electrical@gmail.com)

‡ Corresponding Author; Pushpa Gaur, Department of Electrical Engineering, National Institute of Technology Silchar, Assam, India, 788010,

Tel: +91 9101638607, pushpa.electrical@gmail.com

Received: 17.05.2018 Accepted: 27.06.2018

**Abstract-** This paper presents a load frequency control scheme with the integration of Vehicle-to-grid (V2G) which can enhance the system dynamics under load fluctuations. For this, a detailed multi-area multi-source system is designed with a solar-thermal and a thermal unit in Area1, a gas and thermal unit along with an electric vehicle (EV) fleet in Area2, and two thermal units and an EV fleet in Area3. The thermal units are a single reheat turbine type, and appropriate generation rate constraints are considered for thermal and gas units. The application of Two Degree of Freedom Proportional-Integral-Derivative (2DOF-PID) controller has been made as a secondary controller in all the control areas. A new nature inspired optimization technique called as Wind Driven Optimization is employed for simultaneous optimization of the controller gains and parameters. Comparison of 2DOF-PID controller with classical controllers reveals the superiority of the former under nominal system conditions. The impact of V2G into the system is tested, which proves that the magnitude and numbers of oscillations of the system response is reduced when it encounters load fluctuations. The robustness of the optimized gains and parameters of the 2DOF-PID controller have been verified by carrying out sensitivity analysis under different system conditions.

**Keywords** Vehicle-to-grid; Generation rate constraint; Load frequency control; Wind Driven Optimization; 2DOF-PID controller.

## Nomenclature

$f$	nominal frequency of system (Hz),
*	represents optimum value,
$i$	subscript referred to area $i$ (1, 2, 3),
$T_{sgi}$	Steam governor's time constant (s),
$T_{ti}$	Turbine's time constant (s),
$K_{ri}$	Reheat coefficient of steam turbine,
$T_{ri}$	Reheat time constant of Steam turbine (s),
$K_s$	Gain of solar field,
$T_s$	Time constant of solar field (s),
$T_{cdi}$	Gas turbine compressor discharge volume-time constant (s),
$X_{ci}$	Gas turbine speed governor lead time constant of (s),
$Y_{ci}$	Gas turbine speed governor lag time constant of (s),

$c_{gi}$	Valve positioner of gas turbine,
$b_{gi}$	Valve positioner gas turbine constant of (s),
$T_{fci}$	Time constant of gas turbine fuel (s),
$T_{cri}$	Time delay of gas turbine combustion reaction (s),
$H_i$	Inertia constant of area $i$ (s),
$R_i$	Speed regulation parameter of governor of area $i$ ,
$B_i$	frequency bias constant of area $i$ ,
$K_T$	Participation factor of thermal unit,
$K_{EV}$	Gain of electric vehicle unit,
$T_{EV}$	Time constant of electric vehicle unit (s),
$K_G$	Participation factor of gas unit.

## 1. Introduction

In recent years, there has been a sudden rise in electric power demand, which has forced the electrical power

generation utilities to employ techniques for efficient power generation. It proves to be a tough challenge to continue meeting this ever growing demand of power. Hence, in this race of generation and demand, it is always generation which follows load. There always must be a balance between power energy demand and power generation, and if there is an imbalance in these two the system experiences fluctuations in frequency. For stable operations in an interconnected power system, it is very essential to maintain constant frequency and constant tie line power flow [1]. This is the job of load frequency control (LFC) to maintain this balance in the system by minimizing the area control errors.

With the alarming increase in pollution and hazards caused by the conventional power plants, the researchers are now diverting towards more and more utilization of non-conventional power energy sources. However, this may give rise to some problems like fluctuations in frequency and system voltage. Battery energy storage system (BESS) plays an important role in overcoming these kinds of difficulties and has been utilized by several researchers. One such highly recommended BESS nowadays is the implementation of vehicle-to-grid (V2G) based on the concept of controlling the charging and discharging between the vehicle and the power system.

The literature survey reveals that there are many studies available on LFC of multi-area interconnected power system. Elgard and Fosha presented the idea of modelling of integrated two area thermal power system [2]. Many researchers have carried forward this idea of modelling thermal units and performed LFC. In [3] the authors studied a two area thermal system and studied LFC under a deregulated environment with the effect of bilateral contract. Nanda et al. [4] did LFC of a hydrothermal system with the use of conventional controllers like Integral and Proportional-Integral controllers, with the utilization of mechanical governors in the thermal units. The authors in [5] have presented effect of including renewable sources in the existing thermal system. Most of the LFC studies have been done for thermal and hydrothermal systems, and not much have been done in gas thermal power plants. With the evolution of power systems, integration of different types of generating unit in a single area have come into existence, which is popularly known as multi-source power system. Many researchers are now working in LFC of multi area multi-source involving different types of scenarios, one of which is deregulation [6-8]. Bhowmik et al. [9] studied the impact of incorporation of wind power generation source in a system in evaluating the individual generator contribution to the system. Similarly many other researchers [10-13] have studied the addition of renewable energy sources under different scenarios and in different arena. Literature shows that researchers nowadays are moving towards the application of renewable energy sources like solar, wind, etc. Modelling of solar thermal power generation of parabolic trough collector type has been attempted in [14]. With the growing emphasis of BESS, and V2G technologies, which is also one kind of BESS, many studies are being carried out to evaluate the impact of its integration with the conventional power system [15-20]. Various control strategies have been adopted and different scenarios have been explored by many.

For stabilizing fluctuations in tie line power flow and system frequency, controllers of different variety have been employed by various researchers. With less system complexity in conventional systems, classical controllers like Proportional-Integral-Derivative, Proportional-Integral and Integral controllers were used by a number of researchers. But with the increasing complexity in power systems, these controllers fail to perform well and hence there is a need to explore more options for controllers, like two Degree of Proportional-Integral-Derivative (2DOF-PID) [21]. Several artificial intelligent controllers like fuzzy controllers, neural network controllers have also been employed by few [22-24], but more time is required for setting the rules in fuzzy, and training the neurons in case of neural network. Fractional order controller known as fractional order PID is also utilized for LFC of multi-area systems [25]. But there are many parameters to be taken care of in the fractional order PID controller which makes it time consuming. 2DOF-PID has many advantages over other controllers discussed above and hence provides scope for further utilization.

The performance of controllers in a system depends upon the values of controller gains. To obtain the values of gain various optimization techniques have been used by researchers. Classical techniques which are based on trial and error techniques were extensively used in AGC in most of the literatures when the numbers of parameters to be optimized are very few. In the later stages in AGC of multi-area system where number of parameters to be optimized are more, various heuristic algorithms have been used for optimization. Heuristic techniques such as genetic algorithm (GA) [26], particle swarm optimization (PSO) [27, 28], bacteria foraging (BFO) [29], artificial bee colony algorithm (ABC) [30], firefly algorithm (FA) [31], etc. have been applied in AGC for simultaneous optimization of number of parameters of controllers. An optimization technique inspired by nature called as Wind Driven Optimization has been utilized by Bayraktar et al. [32] and by Singh et al. [33] in electromagnets and WDM channel allocation algorithm respectively. Its utility is yet to be analysed for LFC of multi area system. Hence, this provides a new scope for further investigation. In view of the survey done above the main objectives of this work are:

- 1) Modelling of a three area multi-source power system with the integration of solar-thermal and electric vehicles (EVs)
- 2) Application of 2DOF-PID controller and its comparison with other classical controllers like PID, PI, and I under step load perturbation.
- 3) Application of Wind Driven Optimization technique for simultaneous optimization of controller gains and other parameters
- 4) Impact evaluation of including EVs and solar thermal plant in a power system.
- 5) Sensitivity analysis of 2DOF-PID controller to verify robustness of the optimized gains of the best controller.

**2. Methodology**

The methodologies implemented to achieve the objectives cited above includes modelling of multi-area multi-source interconnected power system incorporating electric vehicle fleet and solar-thermal units, the application of 2DOF-PID controller, and the utilization of WDO technique for optimizing the controller gains.

*2.1. Modelling of multi-area interconnected power system*

The system consists of three unequal areas incorporating solar-thermal unit and thermal unit with single reheat turbine in Area1. In Area2 a gas unit and a thermal unit are considered with an electric vehicle (EV) fleet embedded as the third unit. Similarly, Area3 comprises of two thermal units and an EV fleet. The installed capacities of the generating units in the integrated system are in the ratio Area1:Area2:Area3=1:3:5. The transfer function model of the system taken for investigation is given in Fig.1.

The parameters for the other units have been taken from [5, 8, 9] and are given in Appendix. For the thermal system considered in all the three areas, generation rate constraint (GRC) of 3% per minute is assumed to give a more realistic picture to the system. In Area2 a gas system is considered with a GRC of 20% per minute. Every unit consists of speed governing system, turbine and generator.

The area control error (ACE) of each area is given by (1)

$$ACE = B\Delta f + \Delta P_{tie} \tag{1}$$

Where, B is frequency bias.

Vehicle-to-grid (V2G) technology may be defined as an arrangement in which bidirectional flow of electrical energy between vehicle and electrical grid is possible. The integration of EVs with electrical grid is known as V2G. It is observed that almost 92% of the vehicles remain idle at the parking during the peak hours. During this period the

batteries of the vehicles may be connected to the nearby grid through apt communication devices. The main idea behind this technology is to extract power from the idle vehicles during peak hours and many other purposes. The EVs can be made to charge during light load hours and the power flow can be reversed when required.

The control centres send the deviation in power set point, which is sent as control signals in order to control the power outputs of the generating units and EVs. The EVs inject electrical energy into the grid and the capacity of power can be contributed to load frequency control of a power system. The details on EVs are collected with the help of aggregators and are provided to the control centres. The aggregator also receives information on power set point from the control centres and accordingly allocates to EVs. The model of a vehicle-to grid is shown in Fig. 2.

The transfer function of an aggregate EV fleet is given by (2)

$$TF_{EV} = \frac{K_{EV}}{1 + sT_{EV}} \tag{2}$$

Where,  $K_{EV}$  is the gain of EV which is taken to be 1 for the EV fleet to participate in LFC, and  $T_{EV}$  is the time constant of the battery for EV. The value of  $T_{EV}$  is taken to be 1.

As discussed earlier a solar thermal plant is placed in Area1 as one of the two generating units. It is known that solar energy has a wide scope in meeting the ever growing power demand. There are various ways of trapping solar energy. Photovoltaic system and concentrated solar power (CSP) plant are two of them. Many studies have been done on the types of solar collector such as parabolic trough collector, dish-stirling, flat plate collector, etc. The main task of these collectors is to collect the solar energy and focus on the pipelines carrying fluids, so that it gets heated up and is used for the production of steam in the heat exchanger which further can be utilized to rotate the turbine blades.

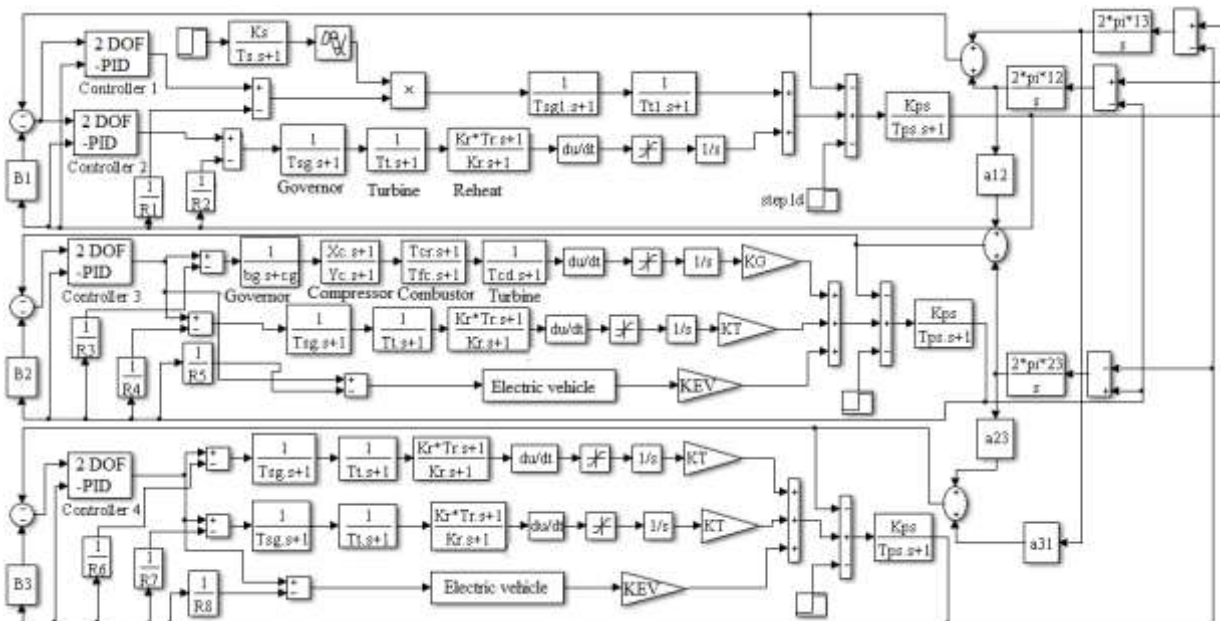


**Fig. 1.** Load frequency control scheme of unequal three area multi-source system comprising of STPP and electric vehicles.

In the presented work, CSP thermal plant is used for electric power generation along with a thermal unit in Area1. The CSP plant consists of a parabolic trough collector type reflectors, which are basically parabola shaped mirrors, the focus of which consists of a pipe (receiver) containing the working fluid. The mirrors are at sun facing positions, which focus the sunrays at the pipe running at the focal point. This heats up the fluid flowing in it, which is then used to boil water to produce steam for running the conventional generators.

The transfer function model for parabolic trough collector type CSP is given by equation (3):

$$TF_{Solar} = \frac{K_s}{T_s \cdot s + 1} \tag{3}$$

The objective function considered for the multi-area multi source power system is integral square error and is represented by equation (4):

$$J = \int_0^T \left\{ (\Delta f_i)^2 + (\Delta P_{tiej-k})^2 \right\} dt \tag{4}$$

Where,  $\Delta f_i$  is the frequency deviation in Area1 and  $\Delta P_{tiej-k}$  is the deviation in tie line power in tie connecting area j and k.

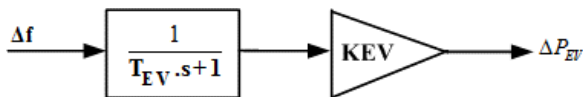


Fig. 2. Transfer function model of vehicle-to-grid

2.2. Two Degree of Freedom Proportional-Integral-Derivative (2DOF-PID) Controller

In control system, degree of freedom is the number of closed loop transfer functions that is liable to be attuned autonomously. 2DOF-PID has several advantages over single degree of freedom controllers. It evaluates a weighted difference signal depending on the set point weights for each of the three actions, that is, proportional, integral and derivative. Its generated output signal is determined by the difference in the reference and measured system output. So finally, the output of the controller will be the sum total of the three above mentioned actions on the respective signals. The schematic diagram of 2DOF-PID controller is shown in Fig. 3.

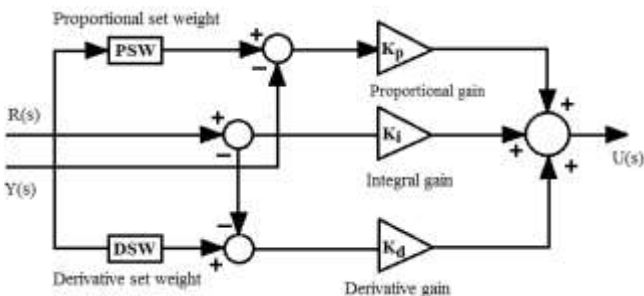


Fig. 3. Schematic diagram of Two Degree of Freedom Proportional-Integral-Derivative (2DOF-PID) Controller

$R(s)$ ,  $Y(s)$  and  $U(s)$  represent reference signal, feedback from the measured system output, and output signal respectively. Proportional, integral and derivative gains are represented respectively by  $K_p$ ,  $K_i$  and  $K_d$ . PSW and DSW are the set point weights of proportional and derivative respectively.

In order to design a controller based on optimization technique, it is necessary to choose an appropriate objective function, founded on the performance criteria depending on the system responses, namely, peak overshoot, rise time, settling time, and steady state errors. Various performance criteria are available in literature, like Integral Squared Error (ISE), Integral Time Squared Error, Integral Absolute Error, and Integral Time Absolute Error. It is very essential in a power system that all oscillations died out as soon as possible. In this paper ISE has been applied as objective function which is given by equation (4).

The controller gains should be small enough to make sure that the area generators are not chasing load deviations of small time durations.

2.3. Wind Driven Optimization Technique

A novel meta-heuristic algorithm inspired by nature called Wind Driven Optimization (WDO) has been proposed by the authors in [24-25]. The wind blows from high pressure region to low pressure region in order to balance the air pressure in our atmosphere with a speed relative to the pressure gradient. Taking assumptions of hydrostatic air balance and vertical movement is weaker than the horizontal movement, the change in pressure as well as the motion of wind can be taken as a horizontal movement. Although, our world is a three-dimensional, the motion of wind takes into account addresses multi-dimensional problems. Furthermore, to derive the operators employed in WDO algorithm, specific assumptions and simplifications are required. The algorithm initializes with Newton’s second law of motion that offers very precise results when utilized to analyse the motion of wind given by equation (5):

$$\rho a = \sum F_i \tag{5}$$

Where, the air density is denoted by  $\rho$ ,  $a$  denotes the acceleration vector, and the forces acting on the mass are denoted by  $F_i$ . The relation between air pressure, density and temperature is given by equation (6):

$$P = \rho RT \tag{6}$$

Where, pressure is denoted by  $P$ , universal gas constants denoted by  $R$  and temperature is denoted by  $T$ .

The motion of wind in any specific path is controlled by four main factors, as specified by equation (5). The friction force ( $F_f$ ) opposes such movement, and is given by equation (7). Gravitational force ( $F_G$ ) given by (8) pulls the particles in the direction of the origin of the coordinate system. Another force called Coriolis force ( $F_c$ ) which is given by (9) happens due to rotation of earth and causes the movement of wind from one dimension to another. Out of all the four factors, pressure gradient force ( $F_{PG}$ ) is the most dominant force that helps in the movement of air and is shown in equation (10).

The implementation of WDO as the movement in one dimension influences the speed in another.

The equations defining the forces are given below, where  $\delta V$  denotes an infinitesimal air volume. Rotation of the earth is represented as  $\Omega$ , gravitational acceleration is denoted by  $g$ , and velocity vector of the wind is denoted by  $u$ .

$$F_F = \rho\alpha u \tag{7}$$

$$F_G = \rho\delta Vg \tag{8}$$

$$F_C = -2\Omega * u \tag{9}$$

$$F_{PG} = -\nabla P\delta V \tag{10}$$

All the above equations defining forces may be added up and put in the right-hand side of the Newton’s second law of motion. The equation formed is given by equation (11):

$$\rho\Delta u = (\rho\delta Vg) + (-\nabla P\delta V) + (-\rho\alpha u) + (-2\Omega * u) \tag{11}$$

The velocity update equation can be derived from the above equation by considering an infinitesimal air particle that moves with the wind. The pressure in equation (6) can be substituted in place of and an assumption of time step to be unity ( $\Delta t = 1$ ) is taken which gives the velocity update equation given by (12):

$$u_{new} = (1 - \alpha)u_{cur} - gx_{cur} + \left( \frac{cu_{cur}^{other\ dim}}{P_{cur}} \right) + \left( \frac{RT}{P_{cur}} | P_{opt} - P_{cur} | (x_{opt} - x_{cur}) \right) \tag{12}$$

The updating of the location of air parcels and their velocity is done in each iteration using equation (12), whereas, updating their position is done by employing equation (13):

$$x_{new} = x_{cur} + (u_{new}\Delta t) \tag{13}$$

Algorithm applied in this paper is shown below:

Steps:

1. Initialize population size, maximum number of iterations, coefficients, boundaries and pressure function definition
2. Assign random position and velocity
3. Evaluate the pressure for all the air parcel

4. Update velocity and check for its limits
5. Update position and check for boundaries
6. If the maximum number of iterations is reached, then stop, otherwise go to step 3.

### 3. Simulation results

An unequal three area multi-source power system with the inclusion of electric vehicles (EVs) and solar-thermal power plant is taken into consideration for the load frequency control (LFC). The study is carried out under nominal system conditions, that is, 1% step load perturbation (SLP) is given as disturbance, loading is considered to be 50%, and inertia constant (H) is taken to be 5s. Two Degree of Freedom Proportional-Integral-derivative (2DOF-PID) controller is used as secondary controller for all the three control areas. A new nature inspired optimization technique known as Wind driven Optimization (WDO) is utilized for the simultaneous optimization of the controller gains and other parameters. A number of studies have been carried out which are explained below.

#### 3.1. Performance comparison of 2DOF-PID, PID, PI and I controllers with 1% SLP in Area1

The performance of Two Degree of Freedom Proportional-Integral-Derivative (2DOF-PID) controller as secondary controller has been compared with other classical controllers like Proportional-Integral-Derivative (PID), Proportional-Integral (PI) and Integral (I) controllers under nominal system conditions. The optimized values of gains of 2DOF-PID, PID, PI and I controllers are formulated in Table 1. Dynamic responses obtained from the analysis of the controllers have been compared and shown in Fig. 4. The values of peak overshoot (POS), peak undershoot (PUS) deviations and settling time (ST) are depicted in Table 2. It is not possible to estimate the values of peak overshoot and overshoot from the figures for PI and I controllers and hence there are blank spaces against the two controllers. Also, the responses for both PI and I do not settle till simulation time  $t$  and hence in Table 2, not settled are abbreviated as NS. It is evident from the critical observation of Table 2 and the responses in Fig. 4 that 2DOF-PID works far better than the other classical controllers under the nominal system conditions.

**Table 1.** Optimum values of gains of secondary controller

Controller	Gains	Optimum values			
		Controller 1	Controller 2	Controller 3	Controller 4
2DOF-PID	$K_{Pi}^*$	0.7069886	0.9794296	0.6515259	0.3635219
	$K_{Ii}^*$	0.6410855	0.2701893	0.0853404	0.6572183
	$K_{Di}^*$	0.5045823	0.4347434	0.1216517	0.2671931
	$b_i^*$	0.2029451	0.2212723	0.0162073	0.3439881
	$c_i^*$	0.9859959	0.1197172	0.6534871	0.8590549
PID	$K_{Pi}^*$	0.2618987	0.7874514	0.2542426	0.2761366
	$K_{Ii}^*$	0.8514382	0.9644587	0.411014	0.8049189
	$K_{Di}^*$	0.9967921	0.3427211	0.4297947	0.3204943
PI	$K_{Pi}^*$	0.3499434	0.1621201	0.5982836	0.1876761
	$K_{Ii}^*$	0.6109586	0.0679927	0.0457267	0.6456427
I	$K_{Ii}^*$	0.3378477	0.6568521	0.4760911	0.5505268

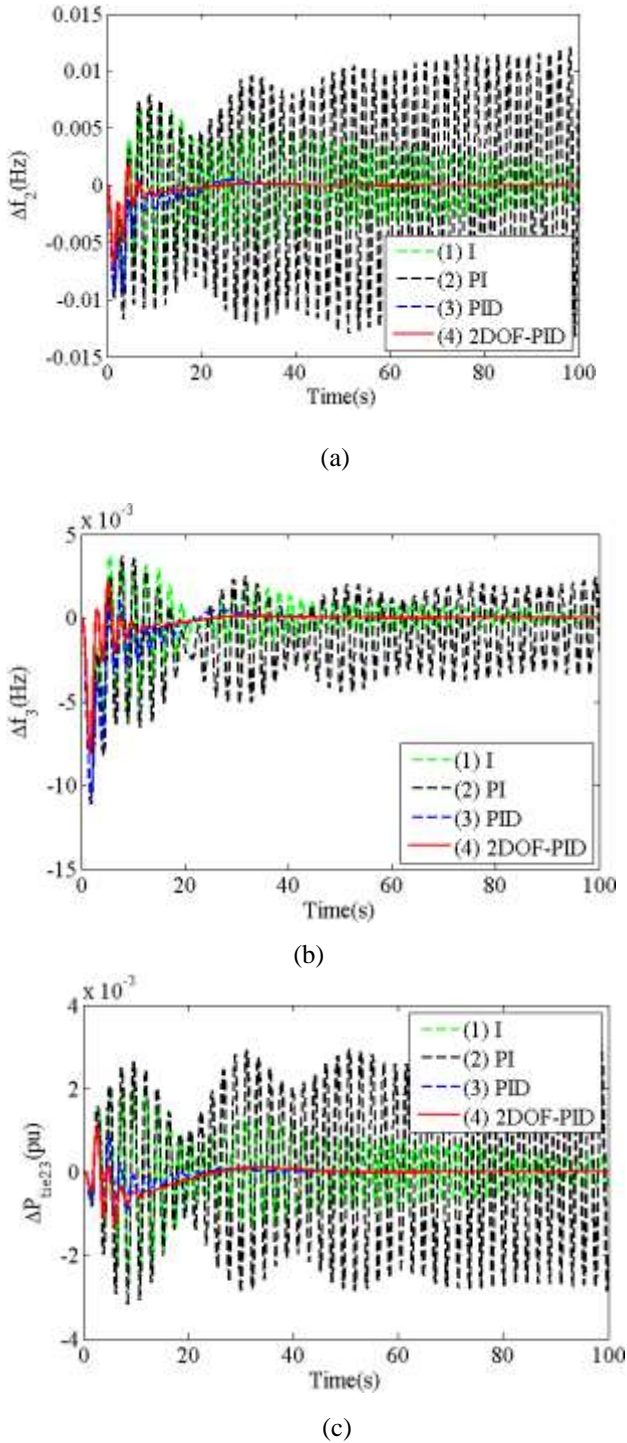


**Fig. 4.** Comparison of responses of 2DOF-PID, PID, PI, and I controllers  
 a)  $\Delta f_2$  vs time  
 b)  $\Delta f_3$  vs. time  
 c)  $\Delta P_{tie23}$  vs. time

From the analysis described above, it is clear that both PI and I controllers do not prove to be efficient in controlling the frequency of complex systems. Hence, for further estimation, these controllers will not be entertained, the best two from above, that is, PID and 2DOF-PID are used for further investigation.

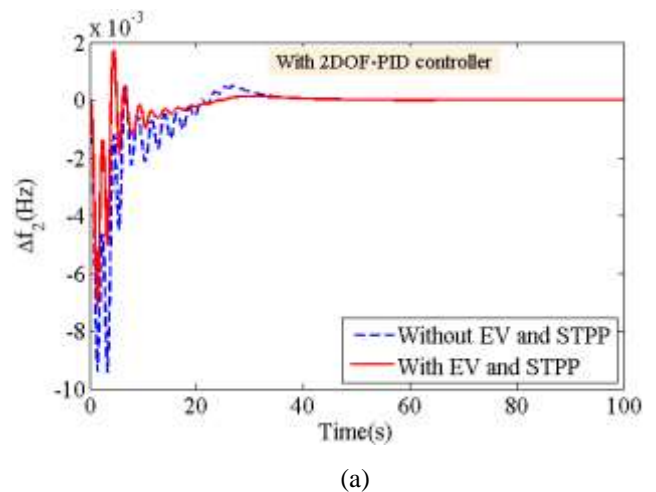
**Table 2.** Values of ST, POS and PUS for Fig. 4

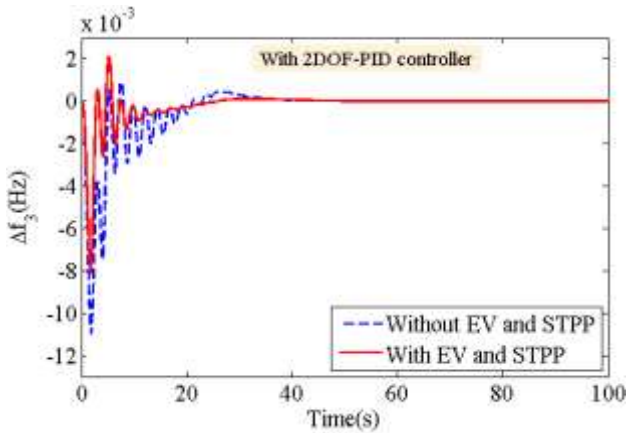
	Controller	Fig. 4a	Fig. 4b	Fig. 4c
Settling time	2DOF-PID	32.99	28.56	49.56
	PID	40.02	42.09	51.21
	PI	NS	NS	NS
	I	NS	NS	NS
Peak overshoot	2DOF-PID	0.001721	0.002113	0.001052
	PID	0.000495	0.0008869	0.00113
	PI	-	-	-
	I	-	-	-
Peak under-shoot	2DOF-PID	0.006939	0.008091	0.001308
	PID	0.009412	0.00978	0.001129
	PI	-	-	-
	I	-	-	-

3.2. Impact assessment of vehicle-to-grid in the system

Electric vehicle (EV) has gained interest from researchers all over the world because of its eco-friendly utility like lower noise pollution and less greenhouse emission. EVs have their own battery and now the vehicle to grid technology has also been developed, which can be connected with the power system to contribute in its operation. Performing as a large battery energy storage system, EVs may participate in stabilizing load fluctuations and frequency variations. In this section, a study has been done to assess the impact of adding EVs to the system and removing them from the system. The dynamic responses obtained for both with and without the EVs in presence of 2DOF-PID and PID as secondary controllers simultaneously are compared and shown in Fig. 5.

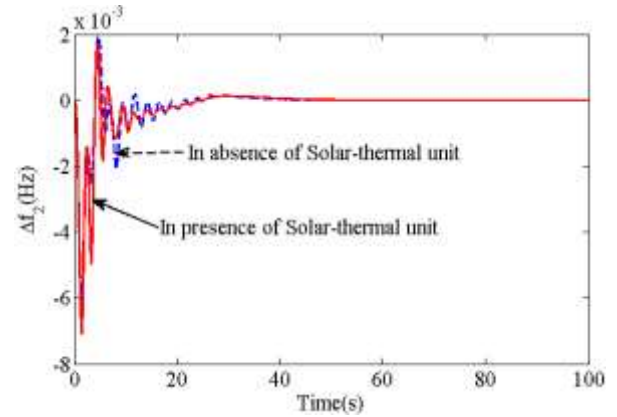
From critical analysis of Fig. 5, it can be concluded that in the absence of EV fleet in the system, there are huge fluctuations in the system in terms of number of oscillations both with 2DOF-PID controller and PID controller. But with the introduction of EV fleet in the system, there is a reduction in the number of oscillations, peak deviations and also the settling time of the dynamic responses.





(b)

**Fig. 5** (a)  $\Delta f_2$  vs. time for 2DOF-PID and PID controllers with and without EVs  
 (b)  $\Delta f_3$  vs. time for 2DOF-PID and PID controllers with and without EVs



(b)

**Fig. 6** (a)  $\Delta f_1$  vs. time for 2DOF-PID and PID controllers with and without Solar-thermal unit  
 (b)  $\Delta f_2$  vs. time for 2DOF-PID and PID controllers with and without Solar-thermal unit

**3.3. Impact valuation of inserting solar thermal power plant in Area1 in the system**

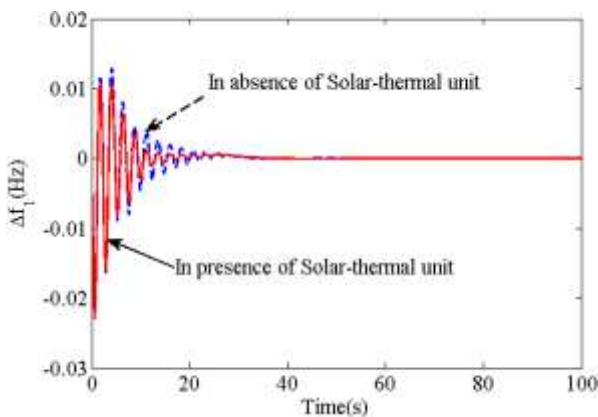
In this section, a solar thermal power plant (STPP) is incorporated in Area1 with the conventional thermal system. Analysis has been carried out to estimate the impact of involving STPP in the system. For this purpose, WDO is used for simultaneously optimizing the gains and other parameters of 2DOF-PID controller. A comparison between the dynamic responses obtained in the absence and presence of STPP has been done and the corresponding responses are shown in Fig. 6. Also, the values of ST, POS and PUS for the responses obtained have been tabulated in Table 3. From critical observation of Fig. 6 and the corresponding Table 3, it is revealed that the system dynamics deteriorate in the absence of STPP in terms of magnitudes and numbers of oscillations, and the time of settling of the dynamics of the system.

**Table 3.** Values of settling time, peak overshoot and peak undershoot for Fig. 6

		Fig. 6(a)	Fig. 6(b)
Settling time (s)	Without STPP	34.13	49.88
	With STPP	31.18	41.08
Peak overshoot	Without STPP	0.01289	0.001957
	With STPP	0.01053	0.001711
Peak undershoot	Without STPP	0.02246	0.006987
	With STPP	0.02246	0.007045

**3.4. Sensitivity analysis**

Sensitivity analysis is carried out to check the robustness of the optimized gains and parameters by varying the model parameters like system loading, magnitude of disturbances and inertia constant (H). In this case the disturbance of the system has been increased from 1% SLP to 2% and 3% SLP and the system dynamics are compared and shown in Fig. 7.



(a)

Similarly, system loading is varied from 50% nominal to 30% and 70% to obtain the system dynamics. Also, analysis with H changed to 4s and 6s from nominal 5s is carried out and the system dynamics are attained, compared. The responses are shown in Fig. 8. Investigation reveals that the responses are almost overlapping; indicating that the optimized gains and parameters are robust enough to withstand any fluctuation in the system conditions and there is no necessity to reset them with variation in system conditions. In each changed condition the 2DOF-PID controller gains are simultaneously optimized using WDO and the results are shown in Table 4.

**Table 4.** Optimum values of 2DOF-PID controller gains at changed system conditions and parameters

Gains	Loading 50%	Loading 30%	Loading 70%	H=6s	H=4s	2% SLP in Area1	3% SLP in Area1
$K_{P1}^*$	0.7069886	0.70688	0.68893	0.69271	0.47911	0.79078	0.67806
$K_{P2}^*$	0.9794296	0.95946	0.96504	0.97859	0.87949	0.97459	0.99925
$K_{P3}^*$	0.6515259	0.62456	0.65259	0.62595	0.52596	0.65258	0.65259
$K_{P4}^*$	0.3635219	0.39371	0.26811	0.57679	0.57178	0.35329	0.35193
$K_{I1}^*$	0.6410855	0.61028	0.51038	0.60721	0.70612	0.56103	0.50389
$K_{I2}^*$	0.2701893	0.29311	0.28781	0.32381	0.29813	0.30819	0.21359
$K_{I3}^*$	0.0853404	0.10325	0.09530	0.09015	0.08035	0.09530	0.18503
$K_{I4}^*$	0.6572183	0.66512	0.66830	0.62713	0.72318	0.61338	0.63863
$K_{D1}^*$	0.5045823	0.42453	0.56895	0.68689	0.58965	0.50473	0.35698
$K_{D2}^*$	0.4347434	0.44356	0.25492	0.45434	0.44345	0.43443	0.37434
$K_{D3}^*$	0.1216517	0.16251	0.21675	0.34136	0.50346	0.12165	0.16571
$K_{D4}^*$	0.2671931	0.29311	0.27131	0.29661	0.39613	0.29113	0.69371
$b_1^*$	0.2029451	0.25415	0.19055	0.26543	0.16543	0.12924	0.14065
$b_2^*$	0.2212723	0.21372	0.23262	0.22397	0.13928	0.27321	0.23982
$b_3^*$	0.0162073	0.00872	0.01651	0.10120	0.01024	0.01277	0.00872
$b_4^*$	0.3439881	0.34589	0.34890	0.43586	0.34988	0.34088	0.34388
$c_1^*$	0.9859959	0.96595	0.99677	0.97894	0.97955	0.59597	0.95915
$c_2^*$	0.1197172	0.09087	0.09027	0.10098	0.08907	0.09082	0.09807
$c_3^*$	0.6534871	0.68317	0.64384	0.62176	0.71761	0.68341	0.63684
$c_4^*$	0.8590549	0.89624	0.94271	0.86132	0.71632	0.86509	0.85609

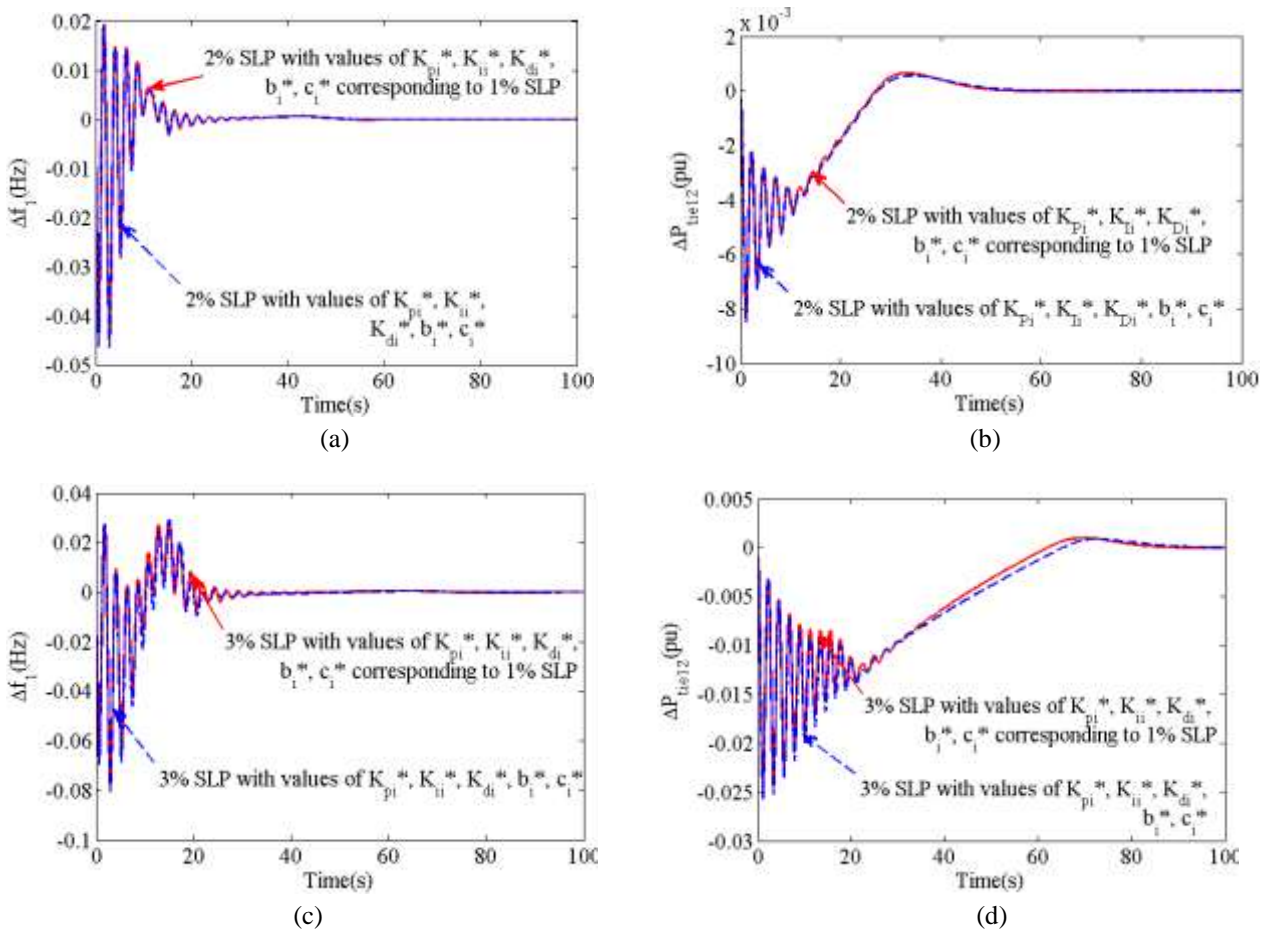


**Fig. 7.** Comparison of  
 a)  $\Delta f_1$  vs. time for 2% SLP in Area1 with  $K_{P1}^*$ ,  $K_{I1}^*$ ,  $K_{D1}^*$ ,  $b_1^*$ ,  $c_1^*$  corresponding to 2% and 1% SLP in Area1  
 b)  $\Delta P_{tie12}$  vs. time for 2% SLP in Area1 with  $K_{P1}^*$ ,  $K_{I1}^*$ ,  $K_{D1}^*$ ,  $b_1^*$ ,  $c_1^*$  corresponding to 2% and 1% SLP in Area1  
 c)  $\Delta f_1$  vs. time for 3% SLP in Area1 with  $K_{P1}^*$ ,  $K_{I1}^*$ ,  $K_{D1}^*$ ,  $b_1^*$ ,  $c_1^*$  corresponding to 3% and 1% SLP in Area1  
 d)  $\Delta P_{tie12}$  vs. time for 3% SLP in Area1 with  $K_{P1}^*$ ,  $K_{I1}^*$ ,  $K_{D1}^*$ ,  $b_1^*$ ,  $c_1^*$  corresponding to 3% and 1% SLP in Area1



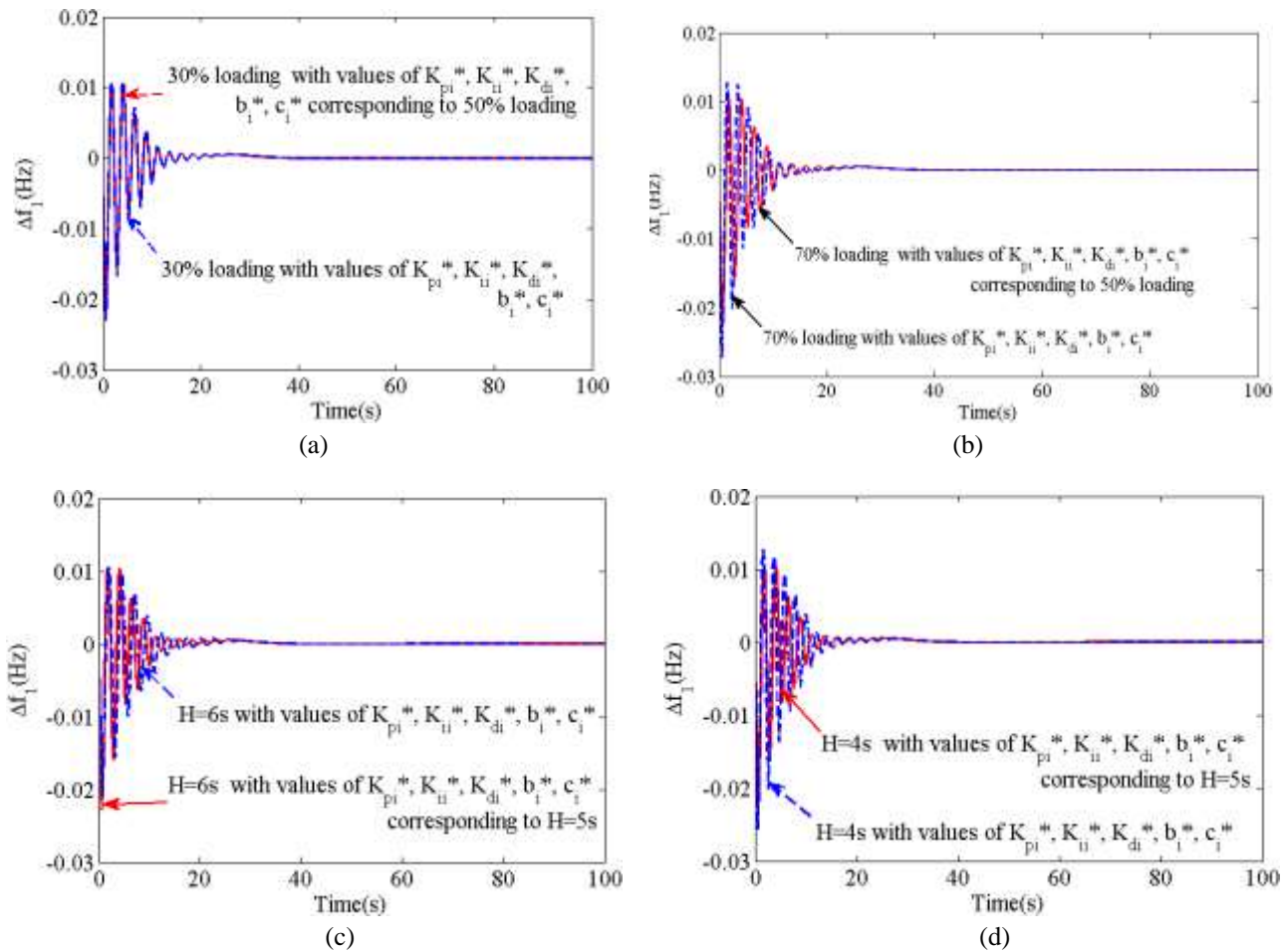


**Fig. 8.** Comparison of  
 a)  $\Delta f_1$  vs. time for 30% loading with  $K_{pi}^*$ ,  $K_{li}^*$ ,  $K_{di}^*$ ,  $b_i^*$ ,  $c_i^*$  corresponding to 30% and 50% loading  
 b)  $\Delta f_1$  vs. time for 70% loading with  $K_{pi}^*$ ,  $K_{li}^*$ ,  $K_{di}^*$ ,  $b_i^*$ ,  $c_i^*$  corresponding to 70% and 50% loading  
 c)  $\Delta f_1$  vs. time for  $H=6s$  with  $K_{pi}^*$ ,  $K_{li}^*$ ,  $K_{di}^*$ ,  $b_i^*$ ,  $c_i^*$  corresponding to  $H=5s$   
 d)  $\Delta f_1$  vs. time for  $H=4s$  with  $K_{pi}^*$ ,  $K_{li}^*$ ,  $K_{di}^*$ ,  $b_i^*$ ,  $c_i^*$  corresponding to  $H=5s$

**4. Conclusion**

Design and analysis of a new LFC scheme with the incorporation of STPP and EV for the management of load fluctuations encountered by the system has been attempted in this paper. The results obtained by using WDO optimized 2DOF-PID controller has been compared with WDO optimized other conventional controller under both nominal and random loading conditions, which reveal the better performance of the former in terms of settling time, and peak deviations. Impact assessment of including STPP and EVs in the system has been made by comparing the responses in their presence and absence. It has been found out that the system behaves superior in the presence of STPP and EVs than that in their absence. Sensitivity analysis discloses the robustness of the optimized gains and other parameters of 2DOF-PID controller, and hence there is no necessity to reset under varying system conditions like magnitude of disturbance, loading and inertia constant.

**Appendix**

Nominal parameters of the systems are:  $f = 60$  Hz;  $T_{sgl} = 0.08s$ ;  $T_{ti} = 0.3s$ ;  $T_{ri} = 10s$ ;  $K_{ri} = 0.5$ ;  $K_{pi} = 120$  Hz/pu MW;  $T_{pi} = 0.08s$ ;  $T_w = 1$  s;  $b_g = 0.5$ ;  $c_g = 1$ ;  $X_c = 0.6$  s;  $Y_c = 1$  s;  $T_{cr} = 0.01$  s;  $T_{fc} = 0.23s$ ;  $T_{cd} = 0.2$  s;  $K_{EV} = 1$ ;  $T_{EV} = 1$ ;  $T_{12} = 0.086$  pu MW/rad;  $H_i = 5s$ ;  $D_i = 8.33 \times 10^{-3}$  pu MW/Hz;  $B_i = -\beta_i = 0.425$  pu MW/Hz;  $R_i = 2.4$  pu Hz/MW; nominal loading = 50%;  $K_s = 1.8$ ;  $T_s = 1.8s$

**References**

[1] O.I. Elgard, Electric energy systems theory', New York, McGraw Hill, 1982.  
 [2] O.I. Elgerd, and C. Fosha, Optimum megawatt frequency control of multi-area electric energy systems, IEEE Trans. Power App. Syst., Vol. 89, No. 4, pp. 556–563, 1970.  
 [3] V. Donde, M. A. Pai, and Ian A. Hiskens, "Simulation and Optimization in an AGC System after Deregulation", IEEE Trans. Power Syst., Vol. 16, No. 3, pp. 481-489, 2001.

- [4] J. Nanda, A. Mangla, and S. Suri, "Some new findings on automatic generation control of an interconnected hydrothermal system with conventional controllers", *IEEE Trans. Energy Convers.*, Vol. 21, No. 1, pp. 187-193, 2006.
- [5] Julian Patino, and Felipe Valencia, Jairo Espinosa, "Sensitivity Analysis for Frequency Regulation in a Two-area Power System", *Int. J. of Renewable Energy Research*, Vol.7, No.2, 2017
- [6] A. K. Barisal, "Comparative performance analysis of teaching learning based optimization for automatic load frequency control of multi-source power systems", *Int. J. of Electrical Power & Energy Systems*, Vol. 66, pp. 67-77, 2015.
- [7] Kazem Zare, Mehrdad Tarafdar Hagh, and Javad Morsali, "Effective oscillation damping of an interconnected multi-source power generation", *Int. J. of Electrical Power & Energy Systems*, Vol. 65, pp. 220-230, 2015.
- [8] K. P. Singh Parmar, S. Majhi, and D. P. Kothari, "Load frequency control of a realistic power system with multi-source power generation", *Int. J. of Electrical Power & Energy Systems*, Vol. 42, No. 1, pp. 426-433, 2012.
- [9] D. Bhowmik, and A. K. Sinha, "Impact Valuation of all Connected Generators Separately by Power Sharing Approach in the Wind Incorporated System", *Int. J. of Renewable Energy Research*, Vol.7, No. 2, 2017.
- [10] U. M. Choi, K. B. Lee, and Frede Blaabjerg, "Power electronics for renewable energy systems: Wind turbine and photovoltaic systems", *Renewable Energy Research and Applications (ICRERA)*, 2012 International Conference on. IEEE, 2012.
- [11] Ziadi, Zakaria, et al., "Real time voltage control of unbalanced distribution systems with photovoltaic generation", *Renewable Energy Research and Applications (ICRERA)*, 2012 International Conference on. IEEE, 2012.
- [12] Morel, Jorge, et al., "Contribution of a hydrogen storage-transportation system to the frequency regulation of a microgrid", *Renewable Energy Research and Applications (ICRERA)*, 2015 International Conference on. IEEE, 2015.
- [13] Atia, Raji, and Noboru Yamada, "Distributed renewable generation and storage systems sizing in deregulated energy markets", *Renewable Energy Research and Applications (ICRERA)*, 2015 International Conference on. IEEE, 2015.
- [14] J. Buzs, "Block-oriented modelling of solar-thermal system", PhD dissertation, Mechanical Engineering, Szent Istvn University (Hungary) 2009.
- [15] T. N. Pham, H. Trinh, and L. V. Hien, "Load frequency control of power systems with electric vehicles and diverse transmission links using distributed functional observers", *IEEE Trans. On Smart Grid*, Vol. 7, No. 1, pp. 238-252, 2016.
- [16] M. Datta, and T. Senjyu, "Fuzzy Control of Distributed PV Inverters/Energy Storage Systems/Electric Vehicles for Frequency Regulation in a Large Power System", *IEEE Trans. On Smart Grid*, Vol. 4, No. 1, pp. 479-488, 2013.
- [17] S. Vachirasricirikul, and I. Ngamroo, "Robust LFC in a Smart Grid With Wind Power Penetration by Coordinated V2G Control and Frequency Controller", *IEEE Trans. on Smart Grid*, Vol. 5, No. 1, pp. 371-380, 2014.
- [18] Taisuke Masuta, and Akihiko Yokoyama, "Supplementary Load Frequency Control by Use of a Number of Both Electric Vehicles and Heat Pump Water Heaters", *IEEE Transactions on Smart Grid*, Vol. 3, No. 3, pp. 1253-1262, 2012.
- [19] Seyedmahdi Izadkhast, Pablo Garcia-Gonzalez, Pablo Frias, Laura Ramirez-Elizondo, and Pavol Bauer, "An Aggregate Model of Plug-in Electric Vehicles Including Distribution Network Characteristics for Primary Frequency Control", *IEEE Transactions on Power Systems*, Vol. 31, No. 4, pp. 2987-2998, 2016.
- [20] Hongming Yang, C. Y. Chung, and Junhua Zhao, "Application of Plug-In Electric Vehicles to Frequency Regulation Based on Distributed Signal Acquisition Via Limited Communication", *IEEE Transactions on Power Systems*, Vol. 28, No. 2, pp. 1017-1026, 2013.
- [21] R. K. Sahu, S. Panda, U. K. Rout, and D. K. Sahoo, "Teaching learning based optimization algorithm for automatic generation control of power system using 2-DOF PID controller", *Int. J. of Electrical Power & Energy Systems*, Vol. 77, pp. 287-301, 2016.
- [22] C. S. Chang, and W. Fu, "Area load frequency control using fuzzy gain scheduling of PI controllers", *Electr Power Syst Res*, Vol. 42, pp. 145-52, 1997.
- [23] M. K. Debnath, S. Sinha, and R. K. Mallick, "Automatic Generation Control Including Solar Thermal Power Generation with Fuzzy-PID Controller with Derivative Filter", *Int. J. of Renewable Energy Research*, Vol.8, No.1, March, 2018
- [24] A. Pappachen, and A. Peer Fathima, "Load frequency control in deregulated power system integrated with SMES-TCPS combination using ANFIS controller", *Int. J. of Electrical Power & Energy Systems*, Vol. 82, pp. 519-534, 2016.
- [25] A. Zamani, S. M. Barakati, and Saeed Yousofi-Darmian, "Design of a fractional order PID controller using GBMO algorithm for load-frequency control with governor saturation consideration", *ISA Transactions*, Vol. 64, pp. 56-66, 2016.
- [26] E. Nikmanesh, O. Hariri, H. Shams, and M. Fasihozaman, "Pareto design of Load Frequency Control for interconnected power systems based on multi-objective uniform diversity genetic algorithm (MUGA)", *Int. J. of Electrical Power & Energy Systems*, Vol. 80, pp. 333-346, 2016.

- [27] H. Gozde, and M. C. Taplamacioglu, "Automatic generation control application with craziness based particle swarm optimization in a thermal power system", *Int J Electr Power Energy Syst*, Vol. 33, No. 1, pp. 8–16, 2011.
- [28] Zadeh, Alimorad K., et al., "Optimized day-ahead hydrothermal wind energy systems scheduling using parallel PSO", *Renewable Energy Research and Applications (ICRERA)*, 2012 International Conference on. IEEE, 2012.
- [29] S. S. Dhillon, J. S. Lather, and S. Marwaha, "Multi objective load frequency control using hybrid bacterial foraging and particle swarm optimized PI controller", *Int. J. of Electrical Power & Energy Systems*, Vol. 79, pp. 196-209, 2016.
- [30] K. Naidu, H. Mokhlis, and A. H. A. Bakar, "Multiobjective optimization using weighted sum Artificial Bee Colony algorithm for Load Frequency Control", *Int. J. of Electrical Power & Energy Systems*, Vol. 55, pp. 657-667, 2014.
- [31] P. C. Pradhan, R. K. Sahu, and S. Panda, "Firefly algorithm optimized fuzzy PID controller for AGC of multi-area multi-source power systems with UPFC and SMES", *Engineering Science and Technology, an International Journal*, Vol. 19, No. 1, pp. 338-354, 2016.
- [32] Z. Bayraktar, M. Komurcu, Jeremy A. Bossard, and Douglas H. Werner, "The Wind Driven Optimization Technique and its Application in Electromagnetics", *IEEE Transactions on Antennas and Propagation*, Vol. 61, No. 5, pp. 2745-2757, 2013.
- [33] P. K. Singh, and N. Gupta, "A Wind Driven Optimization Based WDM Channel Allocation Algorithm", *International Journal of Innovative Research in Science, Engineering and Technology*, Vol. 5, No. 7, pp. 12073-12080, 2016.